



This is a repository copy of *Dynamics of a two degree of freedom vibro-impact system with multiple motion limiting constraints*.

White Rose Research Online URL for this paper:
<http://eprints.whiterose.ac.uk/79671/>

Version: Accepted Version

Article:

Wagg, D.J. and Bishop, S.R. (2004) Dynamics of a two degree of freedom vibro-impact system with multiple motion limiting constraints. *International Journal of Bifurcation and Chaos*, 14. 119 - 140. ISSN 0218-1274

<https://doi.org/10.1142/S0218127404009223>

Reuse

Unless indicated otherwise, fulltext items are protected by copyright with all rights reserved. The copyright exception in section 29 of the Copyright, Designs and Patents Act 1988 allows the making of a single copy solely for the purpose of non-commercial research or private study within the limits of fair dealing. The publisher or other rights-holder may allow further reproduction and re-use of this version - refer to the White Rose Research Online record for this item. Where records identify the publisher as the copyright holder, users can verify any specific terms of use on the publisher's website.

Takedown

If you consider content in White Rose Research Online to be in breach of UK law, please notify us by emailing eprints@whiterose.ac.uk including the URL of the record and the reason for the withdrawal request.



eprints@whiterose.ac.uk
<https://eprints.whiterose.ac.uk/>

**DYNAMICS OF A TWO DEGREE OF FREEDOM VIBRO-IMPACT SYSTEM WITH
MULTIPLE MOTION LIMITING CONSTRAINTS**

D. J. Wagg *

*Department of Mechanical Engineering, University of Bristol, Queens Building,
University Walk, Bristol BS8 1TR, U.K.*

AND

S. R. BISHOP

*Centre for Nonlinear Dynamics and its Applications, University College London,
Gower Street, London WC1E 6BT, U.K.*

May 3, 2013

Abstract

We consider the dynamics of impact oscillators with multiple degrees of freedom subject to more than one motion limiting constraint or stop. A mathematical formulation for modelling such systems is developed using a modal approach including a modal form of the coefficient of restitution rule. The possible impact configurations for an N degree of freedom system are considered, along with definitions of the impact map for multiply constrained systems. We consider sticking motions which occur when a single mass in the system becomes stuck to an impact stop, and discuss the computational issues related to computing such solutions. Then using the example of a two degree of freedom system with two constraints we describe exact modal solutions for the free flight and sticking motions which occur in this system. Numerical examples of sticking orbits for this system are shown and we discuss identifying the region, S in phase space where these orbits exist. We use bifurcation diagrams to indicate differing regimes of vibro-impacting motion for two different cases; firstly when the stops are both equal and on the same side (i.e. the same sign) and secondly when the stops are unequal and of opposing sign. For these two different constraint configurations we observe

*Author for correspondence: david.wagg@bristol.ac.uk

qualitatively different dynamical behavior, which is interpreted using impact mappings and two dimensional parameter space.

Running title: Two DOF impact oscillators with multiple constraints

1 Introduction

In this paper we consider the dynamics of multi-degree of freedom impact oscillators subject to multiple motion limiting constraints. Such impact oscillators consist of a system of coupled masses, where the motion of more than one of the masses is restricted by a series of impact stops. Such systems have a range of applications as, for example, in machines with clearance and backlash [Theodossiades & Natsiavas 2001]. However, in general throughout the associated literature on multi-degree of freedom impact systems, the inclusion of only a single motion limiting constraint predominates. This said, some authors have considered two constraints placed an equal distance either side of an oscillating mass, e.g. Shaw & Shaw [1989], Hogan & Homer [1999]. In this study we will consider the more general case of variable constraints applied to a number of the masses in the system.

The majority of studies carried out on multi-degree of freedom impact oscillators have focused on two-degree of freedom impact oscillator systems. For example, such systems have been studied in relation to impact damper systems Masri [1972], Chatterjee *et al.* [1995], with respect to bifurcations and the onset of chaotic motion [Shaw & Shaw 1989], and the dynamics of rotor bearings [Neilson & Gonsalves 1993].

The effect of an impact damper on a general multi-degree of freedom system has been investigated by Nigm & Shabana [1983]. Higher degree of freedom impact systems have also been considered by Cusumano & Bai [1993], who consider the dynamics associated with a ten degree of freedom impact oscillator and Babitsky [1998] who considers multi-degree of freedom and elastic systems subject to vibro-impact. Periodic impacting motions which occur in multi-degree of freedom impact systems with a single impact stop have been studied by Natsiavas [1993] and Pun *et al.* [1998]. Natsiavas [1993] extends the semi-analytical method for finding period(1, n) solutions developed for single degree of freedom impact oscillators by Shaw & Holmes [1983] to multi-degree of freedom impact oscillators. Luo & Xie [1998] use this approach combined with center manifold theory to study the Hopf bifurcations which occur in a two degree of freedom impact system with a single impact stop. Similar studies on Hopf bifurcations and quasi-periodic solutions have been

carried out by Wen [2001] and Luo & Xie [2002].

Chatter and sticking in single degree of freedom impact oscillators has been considered by Budd & Dux [1994] and in two degree of freedom systems by Wagg & Bishop [2001]. The behavior of periodic sticking motions in both single and multi degree of freedom systems is considered by Toulemonde & Gontier [1998]. In addition the sticking phenomena discussed here have similar properties to the sliding orbits in relay feedback systems described by Di Bernardo *et al.* [2001]. There are also some similarities with stick–slip systems such as those discussed by Galvanetto [2001].

In common with previous authors we consider the example of a two degree of freedom impact oscillator, however in this case the system is subject to motion limiting constraints on each of the two masses. In Sec. 2 we develop a mathematical model for more general N degree of freedom systems with multiple motion limiting constraints. Then in Sec. 3 we discuss the issues related to computing solutions to produce numerical simulations for these type of systems. In Sec. 4 we develop explicit solutions for the two degree of freedom system in both free flight and during sticking motion. We also show numerical examples of the dynamics for motion constraints on the same side and opposite sides of the masses. Conclusions are drawn in Sec. 5.

2 Mathematical Model

We consider a generalized N degree of freedom coupled linear oscillator system with N lumped masses which is shown schematically in Fig. 1. The equations of motion for the coupled masses can be expressed as

$$m_i \ddot{x}_i + c_i(\dot{x}_i - \dot{x}_{i-1}) + c_{i+1}(\dot{x}_i - \dot{x}_{i+1}) + k_i(x_i - x_{i-1}) + k_{i+1}(x_i - x_{i+1}) = f_i(t), \quad (1)$$

for $i = 1, 2, \dots, N - 1$ and

$$m_N \ddot{x}_N + c_N(\dot{x}_N - \dot{x}_{N-1}) + k_N(x_N - x_{N-1}) = f_N(t) \quad (2)$$

for $i = N$ [Gladwell 1986]. Here x_i represents the displacement of mass m_i , an overdot is used to represent differentiation with respect to time t and $f_i(t)$ represents the forcing function applied to the i th degree of freedom. These expressions govern the motion while all the displacements x_i are less than some fixed set of values s_i corresponding to the position of the impact stops.

The equations of motion for the coupled masses can be expressed in matrix form as

$$[M]\ddot{\mathbf{x}} + [C]\dot{\mathbf{x}} + [K]\mathbf{x} = \mathbf{f}(t), \quad (x_i - s_i) \leq 0 \quad \forall s_i \geq 0 \quad (3)$$

where $[M], [C], [K]$ are the mass, damping and stiffness matrices respectively, $\mathbf{x} = \{x_1, x_2, \dots, x_N\}^T$ is the displacement vector and $\mathbf{f}(t) = \{f_1, f_2, \dots, f_N\}^T$ the external forcing vector. The coupling between masses occurs via the matrices $[C]$ and $[K]$, which are nondiagonal. The mass matrix $[M]$ is a diagonal matrix. Equation (3) has the dual condition for free flight that $(x_i - s_i) < 0$ for $s_i > 0$ and $(x_i - s_i) > 0$ for $s_i < 0$.

For these systems we assume that the damping matrix $[C]$ is linearly proportional to the stiffness matrix $[K]$, such that Eq. (3) can be decoupled for a set of $[M], [C], [K]$ matrices [Meirovitch 1967]. We will consider the case where $m_j = m$, $c_j = c$, $k_j = k$ for $j = 1, 2, \dots, N$, which is analogous to a commonly used modelling technique, where systems with continuous, uniformly distributed mass and stiffness, are assumed instead to consist of a series of lumped masses. Then Eq. (3) can be written in the form

$$[I]\ddot{\mathbf{x}} + \frac{c}{m}[E]\dot{\mathbf{x}} + \frac{k}{m}[E]\mathbf{x} = \frac{1}{m}\mathbf{f}(t), \quad (x_i - s_i) \leq 0 \quad \forall s_i \geq 0 \quad (4)$$

where $[E]$ is the $N \times N$ coupling matrix

$$[E] = \begin{bmatrix} 2 & -1 & 0 & \dots & 0 \\ -1 & 2 & -1 & \dots & 0 \\ \vdots & \dots & \ddots & \dots & \vdots \\ 0 & \dots & -1 & 2 & -1 \\ 0 & \dots & 0 & -1 & 1 \end{bmatrix}, \quad (5)$$

and $[I]$ is the identity matrix.

The natural frequencies are given by $\omega_{nj} = \sqrt{\lambda_j k/m}$ for $j = 1, 2, \dots, N$ where λ_j are the eigenvalues of matrix $[E]$, and the corresponding normalized eigenvectors ξ_j can be used we can construct a orthogonal modal matrix $[\Psi] = [\{\xi_1\}, \{\xi_2\}, \dots, \{\xi_N\}]$. We can then transform Eq. (4) into a modal form by defining modal coordinates $\mathbf{x} = [\Psi]\mathbf{q}$ where $\mathbf{q} = \{q_1, q_2, \dots, q_N\}^T$, such that

$$[I]\ddot{\mathbf{q}} + \frac{c}{m}[\Lambda]\dot{\mathbf{q}} + \frac{k}{m}[\Lambda]\mathbf{q} = \frac{1}{m}[\Psi]^T\mathbf{f}(t) \quad (6)$$

where $[\Lambda] = [\Psi]^T[E][\Psi]$ is the diagonal matrix of the eigenvalues, λ_j , $j = 1, 2, \dots, N$.

In this modal formulation, we define the vector $\psi_i = \{\Psi_{i1}, \Psi_{i2}, \dots, \Psi_{iN}\}^T$, such that an impact occurs when $\psi_i^T \mathbf{q} = x_i$. Hence Eq. (6) is valid only for $(\psi_i^T \mathbf{q} - s_i) \leq 0 \quad \forall s_i \geq 0$, which is equivalent to the condition that $(x_i - s_i) \leq 0 \quad \forall s_i \geq 0$ for the i th impacting mass.

We consider the system subject to harmonic forcing of the form $\mathbf{f}(t) = \mathbf{A} \cos(\Omega t)$, where $\mathbf{A} = \{A_1, A_2, \dots, A_N\}^T$. Thus we can simplify Eq. (6) such that for each mode

$$\ddot{q}_j + 2\zeta_j \omega_{nj} \dot{q}_j + \omega_{nj}^2 q_j = \frac{\hat{f}_j}{m} \cos(\Omega t), \quad j = 1, 2, \dots, N \quad (7)$$

where $\hat{\mathbf{f}} = [\Psi]^T \mathbf{A}$, $\hat{\mathbf{f}} = \{\hat{f}_1, \hat{f}_2, \dots, \hat{f}_N\}^T$ and $\zeta_j = (c/2)\sqrt{\lambda_j/km}$ is the modal damping coefficient. Equation (7) has the well known exact solution for under-damped oscillations $0 < \zeta_j < 1$

$$q_j = e^{-\zeta_j \omega_{nj}(t-t_0)} (B_i \cos(\omega_{dj}(t-t_0)) + C_i \sin(\omega_{dj}(t-t_0))) + Q_j \cos(\Omega t - \phi_j) \quad (8)$$

where $\omega_{dj} = \omega_{nj} \sqrt{1 - \zeta_j^2}$ is the damped natural frequency. Also

$$Q_j = \frac{\hat{f}_i}{m [(\omega_{nj}^2 - \Omega^2)^2 + (2\zeta_j \Omega \omega_{nj})^2]^{1/2}} \quad (9)$$

is the j th modal transfer function,

$$\phi_j = \arctan \left(\frac{2\zeta_j \Omega \omega_{nj}}{(\omega_{nj}^2 - \Omega^2)} \right) \quad (10)$$

is the j th modal phase and B_i and C_i are arbitrary constants determined from the initial conditions.

2.1 A coefficient of restitution rule for multiple constraints

A coefficient of restitution (COR) rule is used to model the impact process as it provides a computationally simple model which has been shown (for single degree of freedom systems) to have close correlation with physical impact experiments [Thompson & Stewart 2002; Moon & Shaw 1983; Bishop, Thompson & Foale 1996]. We use an instantaneous coefficient of restitution rule which has been shown to be a suitable model for systems where the impact time is "short" compared with the time in between impacts [Wagg, Karpodinis & Bishop 1999].

A single isolated impact occurs when for the i th mass when $x_i = s_i$, while for all other masses $j \neq i: (x_j - s_j) \leq 0 \quad \forall s_j \geq 0$. This type of single impact may be modelled using an instantaneous coefficient of restitution rule [Thompson & Stewart 2002] such that

$$\dot{x}_i(t_+) = -r \dot{x}_i(t_-) \quad x_i = s_i \quad (11)$$

where, t_- is the time just before impact, t_+ is the time just after impact and r is the coefficient of restitution with a value in the range $r \in [0, 1]$.

For systems with multiple constraints, multiple impacts can occur where two or more of the masses impact simultaneously. Therefore we will consider the coefficient of restitution rule in a matrix formulation.

2.1.1 Modal COR rules for systems of degree N

In matrix form the coefficient of restitution rule is

$$\dot{\mathbf{x}}(t_+) = [\mathbf{R}_i] \dot{\mathbf{x}}(t_-) \quad (x_i - s_i) = 0 \quad \text{for } i \in e \quad (12)$$

where $[R]$ is the $N \times N$ diagonal coefficient of restitution matrix and e is an integer vector containing the appropriate indices of the impacting masses. For a system with $n \leq N$ impacting masses $[R_i]$ will have a different form depending on whether a single, multiple or all the masses make contact during the impact process. In fact for any set of n impacting masses the number, n_r , of possible $[R_i]$ matrices will be given by

$$n_r = \sum_{k=1}^n \frac{n!}{k!(n-k)!} \quad (13)$$

This total number of possibilities for $[R_i]$ is made up of three distinct cases.

1. The single impact case, where $x_j = s_j$, for only one of the n masses which could possibly impact. In this case $[R_i] = \text{diag}[\dots, 1, 1, -r, \dots, 1, 1, \dots]$ is a $N \times N$ diagonal matrix with the i th diagonal element equal to $-r$, and all other diagonal elements equal to 1. For a system with n masses which can impact, there are n possible $[R_i]$ matrices for this case.
2. The multiple impact case where *all* masses impact simultaneously, $(x_i - s_i) = 0, \forall i$, the coefficient matrix in Eq. (12) becomes $[R_i] = \text{diag}[\dots -r, -r, -r, \dots]$. For this case to occur $n = N$ and there is only one $[R_i]$ of this type.
3. The multiple impact case where more than one but less than N masses impact simultaneously; $(x_i - s_i) = 0$, for $i \in e$. For this case there are $n_r - n - 1$ possibilities for $[R_k]$, with $1 < n < N$.

In modal form the coefficient of restitution rule, Eq. (12), becomes

$$[\Psi]\dot{\mathbf{q}}(t_+) = [R_i][\Psi]\dot{\mathbf{q}}(t_-), \quad (\psi_i^T \mathbf{q} - s_i) = 0 \quad \text{for } i \in e. \quad (14)$$

This leads to the relation for the modal velocities after impact

$$\dot{\mathbf{q}}(t_+) = [\hat{R}_i]\dot{\mathbf{q}}(t_-), \quad (\psi_i^T \mathbf{q} - s_i) = 0 \quad \text{for } i \in e, \quad (15)$$

where $[\hat{R}_i] = [\Psi]^{-1}[R_i][\Psi]$ is the set of n_r matrices which represents a linear transform of modal velocities just before impact to modal velocities just after impact for the n_r possible impact cases.

We note that for the simultaneous impact case (case 2) we can write

$$\dot{\mathbf{q}}(t_+) = -r[\Psi]^{-1}[I][\Psi]\dot{\mathbf{q}}(t_-), \quad (\psi_i^T \mathbf{q} - x_i) = 0 \quad \forall i, \quad (16)$$

so that

$$\dot{\mathbf{q}}(t_+) = -r\dot{\mathbf{q}}(t_-), \quad (\psi_i^T \mathbf{q} - x_i) = 0 \quad \forall i. \quad (17)$$

So in this case the modal velocities are simply reversed and reduced by a factor of r .

2.1.2 Modal COR rules for systems with $N \leq 2$

There are two exceptions to the modal COR rules presented above, $N = 1$ in which case no modal transform is required and $N = 2$ which is the case we will consider in detail in this paper. The two degree of freedom system is an exception to the general case for N masses because only single or double impacts are possible i.e. from Sec. 2.1 only cases 1 and 2 are possible, case 3 can only occur when $N \geq 2$.

2.2 Impact mappings for systems with multiple constraints

When only a single mass is constrained in a multi-degree of freedom oscillator, an impact map for a multi-degree of freedom impact system can be defined in a similar way to the map for a single degree of freedom system [Wagg & Bishop 2001]. However, for a multiply constrained system we cannot define an impact mapping in this way. Essentially for multiply constrained systems there are two alternatives. Either consider a separate impact map for each of the constrained masses, or consider an impact map from one impact to the next, independent of where the impact occurs in the system.

In the first case a series of impact maps are formed by considering the hypersurfaces, Σ_i , in the complete phase space defined by the impact stops $x_i = s_i$ such that $\Sigma_i = \varphi_i \in \mathbb{R} \times v_i \in \mathbb{R}$ where φ_i is the phase at impact; time modulo the forcing frequency and v_i represents the velocity of mass i at impact. This is a Poincaré type section through the flow, in phase space $G = \mathbb{R}^{2N+1}$ for a N degree of freedom oscillator. The i th impact map is formed by intersections between Σ_i and the flow. Using this approach there will be n separate impact maps $P_i : (\varphi_i, v_i)_k \mapsto (\varphi_i, v_i)_{k+1}$. We define these mappings as individual impact mappings, as they relate subsequent impacts of individual masses irrespective of other impacts occurring in the system.

The second possible approach to defining an impact mapping for a multiply constrained impact oscillator is to define a global impact map, which relates each impact in the system sequentially regardless of which mass is impacting. In this case we define a hypersurface, Υ which is the union of the local impact map hypersurfaces Σ_i such that $\Upsilon = \bigcup \Sigma_i$. The global mapping is $P_g : (\varphi_I, v_I)_k \mapsto (\varphi_I, v_I)_{k+1}$ where v_I is the velocity of the impacting mass and φ_I the corresponding phase.

These impact mappings can be used to identify periodic and non-periodic behavior in the multiply constrained system example. For the examples computed in Sec. 4.5.1 we have used only the individual impact mappings as they show the dynamics most clearly.

2.3 Sticking motion

In this work we consider sticking motions when one of the masses (the p th say) is held motionless against the stop for a finite period of time, while the other masses in the system continue to oscillate. Sticking motions can occur in multi-degree of freedom impact oscillators after a complete chatter sequence has occurred [Budd & Dux 1994; Wagg & Bishop 2001]. A chatter sequence becomes complete when the time between two successive impacts, $\delta t \rightarrow 0$, while at the same time the force acting on mass p holds it against the impact stop. Once sticking occurs the dynamics of the system are governed by a reduced, $N - 1$ set of governing equations

$$[I]\ddot{\hat{\mathbf{x}}} + \frac{c}{m}[\hat{E}]\dot{\hat{\mathbf{x}}} + \frac{k}{m}[\hat{E}]\hat{\mathbf{x}} = \frac{1}{m}\hat{\mathbf{f}}(t), \quad (x_i - s_i) \leq 0 \quad \forall s_i \geq 0 \quad \forall i \neq p \quad (18)$$

in which $\hat{\mathbf{x}}$ is an $(N - 1) \times 1$ vector $\hat{\mathbf{x}} = \{x_i \in \mathbf{x} : i \neq p\}$, and \hat{E} is an $(N - 1) \times N$ matrix formed by excluding the p th row from E .

When (single mass) sticking occurs the dimension of the overall phase space is reduced by 2. As a result the reduced phase space for Eqns. (18) becomes $\hat{G} = \mathbb{R}^{N+1-2} = \mathbb{R}^{N-1}$. \hat{G} is the space in which (single mass) sticking motions can evolve, in order to reach a sticking solution certain conditions must be satisfied. First, chatter must be complete, i.e if δt is the time between impacts, $\delta t \rightarrow 0$ as chatter becomes complete. Secondly, when chatter is complete, the force acting on the sticking mass, F_p , must hold it against the stop, which is equivalent to the condition $F_p s_p > 0$. Di Benardo *et al.* [2001] refer to similar conditions for a relay system as the *reaching conditions*. There is one possible exception to these conditions, that is if a mass comes into contact with the stop with zero velocity and acceleration and simultaneously $F_p s_p > 0$ becomes true. This non-generic case will not be considered here.

To find the force F_p , we substitute $x_p = s_p$ and $\dot{x}_p = 0$ into the p th line of Eq. (4). So for $1 \leq p < N$ from Eq. (1) with all m, c and k values equal

$$F_p = c(\dot{x}_{p-1} + \dot{x}_{p+1}) + k(x_{p-1} + x_{p+1}) + f_p(t) + 2ks_p, \quad (19)$$

and for $p = N$ from Eq. (2),

$$F_p = c\dot{x}_{p-1} + kx_{p-1} + f_p(t) - ks_p. \quad (20)$$

The end of sticking is defined as when F_p changes sign.

As a result, Eqs. (19) and (20) set equal to zero, can be used to define one boundary of the sticking region in the reduced phase space \hat{G} . We can define the region of sticking trajectories as

$S \in \hat{G}$, which is bounded on one side by the exit boundary ∂S defined by $F_p = 0$. However, due to the nature of trajectories reaching sticking we cannot define a unique set of points for the onset of sticking. This will be discussed when we consider the two degree of freedom example in Sec. 4.6.

3 Computing Solutions for Systems with Multiple Constraints

Before considering a detailed numerical example, we discuss briefly the issues related to how to compute solutions for systems with multiple constraints. A flow diagram showing the complete sequence of operations for numerically computing solutions for the two degree of freedom system is shown in Fig. 3. Impact maps are computed by iterating a time series of system states between impact events, starting with arbitrary initial conditions (usually all states set to zero). For this work, simultaneous sticking of both masses has not been observed, and is therefore not required to be dealt with numerically.

3.1 *Motion without sticking*

In between two consecutive impacts, since the system considered here is linear, we can find the exact solution for any N degree of freedom system with constant mass, stiffness and viscous damping explicitly via the modal equations; Eqs. (7). However for these systems the time of impact cannot be found analytically [Shaw & Holmes 1983], and as a result this is computed numerically using (in this case) a secant type root finding method. For systems with multiple constraints, the impact conditions are checked at each time step, Δt , to see if any single impacts or multiple impacts have occurred. Depending on whether a single or multiple impact occurs, the appropriate $[\hat{R}_i]$ matrix is then used to apply the coefficient of restitution rule to the system, after which the initial conditions are reset and the time stepping using exact solutions begins again.

3.2 *Motion including sticking*

Computing sticking solutions is a more complex process. Sticking occurs after a complete chatter sequence, with the condition that the mass is being held against the impact stop $F_p s_p > 0$. Numerically we can identify sticking by monitoring the interval between successive impacts, δt , and the force on the mass towards the stop [Cusumano & Bai 1993]. Once δt drops below a threshold level ($4\Delta t$ in these simulations), and providing the force on the mass is acting against the stop $F_p s_p > 0$, we assume that the mass is stuck to the stop. At this point we reset the initial

conditions and compute the solution based on the reduced system, Eq. (18). To detect the end of sticking, we locate the time at which the force changes sign (Eqs. (19) and (20)) and apply the end of sticking conditions (defined for the two degree of freedom example as Eqs. (34) and (39)) which serve as initial conditions for the free motion.

3.3 *Sticking motion with additional impacts*

During sticking of one mass it is possible that another impact in the system may occur. We can deal with this in a similar way to the motion without sticking. Using the exact sticking solutions we first root find to locate the exact time of impact, then apply the coefficient of restitution rule which in the $N = 2$ case is just $\dot{x}_+ = -r\dot{x}_-$ i.e. the velocity of the free mass is reversed and reduced by the coefficient of restitution. Finally we reset the initial conditions before time stepping again using the exact sticking solutions.

3.4 *Dealing with simultaneous impacts*

Numerically we define a simultaneous impact as occurring when all impact conditions become true simultaneously within one time step, Δt . Within the time step the time of impact is taken as the time value which minimizes the error of each of the displacement error values, $|x_i - s_i|$, $\forall i$. Once this value is found, the coefficient of restitution rule from case 2 is applied, and the initial conditions recalculated. For numerical simulations computed in this paper it was found that the computational error for finding simultaneous impacts was less than or equal to 5×10^{-4} .

4 A Two Degree of Freedom System Example

We will consider a two degree of freedom impact oscillator with multiple constraints as shown schematically in Fig. 2 (a) and (b). We select the following parameter values: masses $m_1 = m_2 = 1$, stiffness $k_1 = k_2 = 1$, viscous damping $c_1 = c_2 = 0.1$, coefficient of restitution $r = 0.7$. In case Fig. 2 (a) we select stop distances $s_1 = s_2 = 0.3$, and in case Fig. 2 (b) $s_1 = -0.3$, $s_2 = 0.1$. This parameter choice will enable us to investigate a range of dynamical behavior including chaos, periodic motion, chatter and sticking. The choice of $c = 0.1$ and $r = 0.7$ is relevant to the energy loss characteristics of a wide range of mechanical systems. For case (a), the equal stop distances with the same sign, $s_1 = s_2 = 0.3$ is analogous to a flexible element vibrating at a fixed distance from motion limiting constraint. For case (b), the unequal stop distances with

different signs, $s_1 = -0.3$, $s_2 = 0.1$ will provide a counter example which breaks the symmetry of the system. Choosing unity mass and stiffness values gives a simplified relationship between the natural frequency values and the system eigenvalues. As a result the frequency range of interest will be that close to the two natural frequencies for the system, which for this example are $\omega_{n1} = 0.618$ and $\omega_{n2} = 1.618$.

From Eq. (4), the equations of motion for two coupled masses can be expressed as

$$\ddot{x}_1 + \frac{c}{m}(2\dot{x}_1 - \dot{x}_2) + \frac{k}{m}(2x_1 - x_2) = \frac{A_1}{m} \cos(\Omega t), \quad (21)$$

$$\ddot{x}_2 + \frac{c}{m}(\dot{x}_2 - \dot{x}_1) + \frac{k}{m}(x_2 - x_1) = \frac{A_2}{m} \cos(\Omega t). \quad (22)$$

where x_1 represents the displacement of mass m_1 and x_2 the displacement of mass m_2 . When $(x_i - s_i) = 0$ for $i = 1, 2$ an impact occurs and an instantaneous coefficient of restitution rule is applied via Eq. (12). For this system $e = [1, 2]^T$, there are $n = N = 2$ impacting masses, and the number of possible $[R_k]$ matrices, $n_r = 3$. Explicitly the three $[R_k]$ matrices are

$$[R_1] = \begin{bmatrix} -r & 0 \\ 0 & 1 \end{bmatrix}, \quad [R_2] = \begin{bmatrix} 1 & 0 \\ 0 & -r \end{bmatrix}, \quad [R_3] = \begin{bmatrix} -r & 0 \\ 0 & -r \end{bmatrix}. \quad (23)$$

4.1 Nondimensionalization

In this work we have deliberately chosen not to nondimensionalize the governing equations of motion. The main reason for this is that the nondimensionalization cannot be generalized for any N . However, we have selected parameters which give equations which are exactly equivalent to those in a nondimensionalized form. To see this we write Eqs. (21) and (22) in the nondimensionalized form

$$\begin{bmatrix} \mu_m & 0 \\ 0 & 1 \end{bmatrix} \begin{bmatrix} \ddot{\xi}_1 \\ \ddot{\xi}_2 \end{bmatrix} + \begin{bmatrix} 2\zeta_1\sqrt{\mu_m\mu_k} + 2\zeta_2 & -2\zeta_2 \\ -2\zeta_2 & 2\zeta_2 \end{bmatrix} \begin{bmatrix} \dot{\xi}_1 \\ \dot{\xi}_2 \end{bmatrix} + \begin{bmatrix} 1 + \mu_k & -1 \\ -1 & 1 \end{bmatrix} \begin{bmatrix} \xi_1 \\ \xi_2 \end{bmatrix} = \begin{bmatrix} \tilde{f}_1 \\ \tilde{f}_2 \end{bmatrix} \quad (24)$$

where $\mu_m = m_1/m_2$, $\mu_k = k_1/k_2$, $\zeta_1 = c_1/(2m_1\varpi_{n1})$, $\zeta_2 = c_2/(2m_2\varpi_{n2})$, $\varpi_{n1} = \sqrt{k_1/m_1}$, $\varpi_{n2} = \sqrt{k_2/m_2}$, $\omega_1 = \Omega_1/\varpi_{n2}$, $\omega_2 = \Omega_2/\varpi_{n2}$, $\tilde{f}_1 = P_1 \cos(\omega_1\tau)$, $\tilde{f}_2 = P_2 \cos(\omega_2\tau)$, $P_1 = A_1/(k_2x_c)$, $P_2 = A_2/(k_2x_c)$, $\tau = \varpi_{n2}t$ and $\xi = x/x_c$. The nondimensional variable ξ is achieved by dividing displacement, x , by a constant displacement x_c . For single degree of freedom impact oscillators x_c can be chosen as the stop distance s_i or the forcing amplitude A_i/k_i . However, for systems with multiple constraints where there are multiple values for these parameters the choice becomes arbitrary, and therefore we will assume that $x_c = 1$.

We have selected parameter values $m_1 = m_2 = k_1 = k_2 = 1$ and $c_1 = c_2 = 0.1$ which means that in the nondimensionalized case $\mu_m = \mu_k = \varpi_{n1} = \varpi_{n2} = 1$ and $\zeta_1 = \zeta_2 = \zeta = c/2$. So, Eq. (24) becomes

$$\begin{bmatrix} \ddot{\xi}_1 \\ \ddot{\xi}_2 \end{bmatrix} + 2\zeta \begin{bmatrix} 2 & -1 \\ -1 & 1 \end{bmatrix} \begin{bmatrix} \dot{\xi}_1 \\ \dot{\xi}_2 \end{bmatrix} + \begin{bmatrix} 2 & -1 \\ -1 & 1 \end{bmatrix} \begin{bmatrix} \xi_1 \\ \xi_2 \end{bmatrix} = \begin{bmatrix} P_1 \cos(\omega_1 \tau) \\ P_2 \cos(\omega_2 \tau) \end{bmatrix} \quad (25)$$

We can see by inspection that Eq. (25) is exactly equivalent (numerically) to Eq. (4) with $c/m = 2\zeta = 0.1$, $k/m = 1$, $f_1 = P_1 \cos(\omega_1 \tau) = A_1 \cos(\Omega t)$ and $f_2 = P_2 \cos(\omega_2 \tau) = A_2 \cos(\Omega t)$.

4.2 Modal equations

The eigenvalues of the 2×2 coupling matrix $[E]$ are $\lambda_1 = 0.382$ and $\lambda_2 = 2.618$, and the corresponding normalised eigenvectors, $\xi_1 = [0.526, 0.851]^T$ and $\xi_2 = [-0.851, 0.526]^T$, give the mode shapes for the non-impacting system, such that for mode 1 the masses are in phase, and mode 2 the masses are out of phase. Using the modal transform described in Sec. 2, we can express the modal equations of motion for this example as

$$\ddot{q}_1 + 2\zeta_1 \omega_{n1} \dot{q}_1 + \omega_{n1} q_1 = \frac{\hat{f}_1}{m} \cos(\Omega t), \quad (26)$$

$$\ddot{q}_2 + 2\zeta_2 \omega_{n2} \dot{q}_2 + \omega_{n2} q_2 = \frac{\hat{f}_2}{m} \cos(\Omega t). \quad (27)$$

For this example there are two modal impact vectors, $\psi_1 = [\Psi_{11}, \Psi_{12}]$ and $\psi_2 = [\Psi_{21}, \Psi_{22}]$, such that $\psi_1 \mathbf{q} = s_1$ and $\psi_2 \mathbf{q} = s_2$, where $\mathbf{q} = [q_1, q_2]^T$. For the numerical simulations in this paper we set the forcing amplitudes as $A_2 = 0$ and $A_1 = 0.5$ and take initial conditions $q_1(t_0) = q_2(t_0) = \dot{q}_1(t_0) = \dot{q}_2(t_0) = t_0 = 0$. This gives constant values for B_j and C_j in Eq. (8) of

$$B_j = q_j - Q_j \cos(\Omega t_0 - \phi_j), \quad (28)$$

$$C_j = \frac{1}{\omega_{dj}} (\dot{q}_j + \zeta_j \omega_{nj} q_j - \zeta_j \omega_{nj} Q_j \cos(\Omega t_0 - \phi_j) + \omega_{nj} Q_j \sin(\Omega t_0 - \phi_j)), \quad (29)$$

for $j = 1, 2$. These expressions are recalculated after each impact event, with t_0 as the time of impact (i.e. $t_0 = t+$) and $\dot{q}_j(t_0)$ values computed using the appropriate coefficient of restitution rule matrix $[\hat{R}_k]$. These expressions can be used to compute the exact solutions for non sticking solutions, we now consider developing explicit solutions for the sticking cases.

4.3 Explicit solutions for sticking motions

For this two degree of freedom example there are two possible sticking regimes; when $x_1 = s_1$ and when $x_2 = s_2$. Each regime has a reduced set of governing equations with explicit solutions.

4.3.1 Sticking case 1: $x_1 = s_1$

In this case $x_1 = s_1$ and $\dot{x}_1 = 0$, and $\hat{\mathbf{x}} = x_2$, so that the reduced equation of motion, Eq. (22) with $A_2 = 0$, is

$$\ddot{x}_2 + \frac{c}{m}\dot{x}_2 + \frac{k}{m}(x_2 - s_1) = 0, \quad (30)$$

and the force which holds the mass against the stop during sticking, from Eq. (21) is given by

$$F_2 = c\dot{x}_2 + k(x_2 - 2s_1) + A_1 \cos(\Omega t). \quad (31)$$

Equation (30) has the exact solution

$$x_2 = e^{-\hat{\zeta}\hat{\omega}_n(t-t_s)}(C_1 \cos(\hat{\omega}_d(t-t_s)) + C_2 \sin(\hat{\omega}_d(t-t_s))) + s_1, \quad (32)$$

where $\hat{\omega}_n = \sqrt{k/m}$, $\hat{\zeta} = c/2m\hat{\omega}_n$ and $\hat{\omega}_d = \hat{\omega}_n\sqrt{1-\hat{\zeta}^2}$. At the start of the sticking period $t_s = t$ and the constants C_1 and C_2 can be found using the initial conditions $x_1(t_s) = s_1$ and $\dot{x}_1(t_s) = 0$ such that

$$\begin{aligned} C_1 &= (x_2(t_s) - s_1) \\ C_2 &= \frac{1}{\hat{\omega}_d}(\dot{x}_2(t_s) + \hat{\zeta}\hat{\omega}_n(x_2(t_s) - s_1)). \end{aligned} \quad (33)$$

The change from free motion of both masses to one mass sticking represents a reduction in the degree of freedom of the system from 2 to 1. The initial conditions for Eq. (32) can be taken directly from the values of x_2 and \dot{x}_2 immediately prior to a sticking phase when $x_1 = s_1$ and $\dot{x}_1 = 0$. The sticking phase ends when F_2 becomes zero and changes sign at which time $t = t_f$. The initial conditions for the modal coordinates at the end of a sticking phase and the beginning of a free flight phase can be found via the relationship $\mathbf{q}(t_0) = [\Psi]^T \mathbf{x}(t_f)$ which in this case gives

$$\begin{aligned} q_1(t_0) &= s_1\psi_{11} + x_2(t_f)\psi_{21} \\ q_2(t_0) &= s_1\psi_{12} + x_2(t_f)\psi_{22} \\ \dot{q}_1(t_0) &= \dot{x}_2(t_f)\psi_{21} \\ \dot{q}_2(t_0) &= \dot{x}_2(t_f)\psi_{22} \end{aligned} \quad (34)$$

4.3.2 Sticking case 2: $x_2 = s_2$

In this case $x_2 = s_2$ and $\dot{x}_2 = 0$, and $\hat{\mathbf{x}} = x_1$. Using a similar approach to that developed in sticking case 1, the reduced equation of motion is given by

$$\ddot{x}_1 + 2\frac{c}{m}\dot{x}_1 + \frac{k}{m}(2x_1 - s_2) = \frac{A_1}{m} \cos(\Omega t). \quad (35)$$

The force which holds the mass against the stop during sticking is given by

$$F_1 = c\dot{x}_1 + k(x_1 - s_2). \quad (36)$$

Equation (35) has the exact solution

$$x_1 = e^{-2\hat{\zeta}\hat{\omega}_n(t-t_s)}(C_1 \cos(2\omega_d^*(t-t_s)) + C_2 \sin(2\omega_d^*(t-t_s))) + C_3 \cos(\Omega t - \phi^*) - s_2/2, \quad (37)$$

where $\hat{\omega}_n = \sqrt{k/m}$, $\hat{\zeta} = c/2m\hat{\omega}_n$ and $\omega_d^* = \hat{\omega}_n \sqrt{0.5 - \hat{\zeta}^2}$ and t_0 is taken at the start of the sticking period and

$$\begin{aligned} \phi^* &= \arctan\left(\frac{4\hat{\zeta}(\Omega/\hat{\omega}_n)}{2 - \Omega^2/\hat{\omega}_n^2}\right) \\ C_1 &= (x_1(t_s) - C_3 \cos(\Omega t_s - \phi^*) - s_2/2) \\ C_2 &= \frac{1}{\hat{\omega}_d}(\dot{x}_1(t_s) + \hat{\zeta}\hat{\omega}_n(x_2(t_s) - C_3 \cos(\Omega t_s - \phi^*) - s_2/2)) + \Omega C_3 \sin(\Omega t_s - \phi^*) \\ C_3 &= \frac{A_1}{m\sqrt{(2\hat{\omega}_n^2 - \Omega^2) + (4\hat{\zeta}\hat{\omega}_n\Omega)^2}} \end{aligned} \quad (38)$$

As with the preceding case the initial conditions for Eq. (32) can be taken directly from the values of x_1 and \dot{x}_1 immediately prior to a sticking phase when $x_2 = s_2$ and $\dot{x}_2 = 0$. The initial conditions for the modal coordinates at the end of a sticking phase and the beginning of a free flight phase are given by

$$\begin{aligned} q_1(t_0) &= s_2\psi_{21} + x_1(t_f)\psi_{11} \\ q_2(t_0) &= s_2\psi_{22} + x_1(t_f)\psi_{12} \\ \dot{q}_1(t_0) &= \dot{x}_1(t_f)\psi_{11} \\ \dot{q}_2(t_0) &= \dot{x}_1(t_f)\psi_{12} \end{aligned} \quad (39)$$

4.3.3 Comparison of system natural frequencies

It is worth noting that for this system we now have four different damped natural frequencies. During free flight ω_{d1} and ω_{d2} are the system natural frequencies. For the sticking case $x_1 = s_1$, $\hat{\omega}_d$ is the natural frequency of the system, and for $x_2 = s_2$, ω_d^* applies. A summary of the frequency and damping values for the two degree of freedom example is shown in 1.

Table 1: Frequency and damping values for the two degree of freedom system

Free flight	$x_1 = s_1$	$x_2 = s_2$
-------------	-------------	-------------

$\omega_{n1}=0.618$	$\hat{\omega}_n=1$	$\hat{\omega}_n=1$
$\omega_{n2}=1.618$		
$\zeta_1=0.031$	$\hat{\zeta}=0.05$	$\hat{\zeta}=0.05$
$\zeta_2=0.081$		
$\omega_{d1}0.618$	$\hat{\omega}_d=0.999$	$\omega_d^*=0.705$
$\omega_{d2}1.613$		

From table 1 we can see that when $x_2 = s_2$ the damped natural frequency of the system is closer to ω_{n1} than in the $x_1 = s_1$ where it is closer to one which is nearer the midway point between ω_{n1} and ω_{n2} .

4.4 Case (a); equal motion constraints of the same sign

Now we consider the case where both the motion limiting constraints are on the same side of each mass and are equal in magnitude i.e. $s_1 = s_2 > 0$. This configuration is shown schematically in Fig. 2 (a). Using the parameter values $m_1 = m_2 = k_1 = k_2 = 1$, $c_1 = c_2 = 0.1$, $s_1 = s_2 = 0.3$, $r = 0.7$ and $A_2 = 0$, we consider the dynamics of the system for a range of forcing amplitude, A_1 , and forcing frequency, Ω , values. Periodic and non-periodic motions can be identified from observing the impact mapping after any transient dynamics have diminished. As a result we plot bifurcation diagrams for the system using the impact velocities of mass 1 and mass 2 as the forcing frequency is varied. In both diagrams Ω was used as a bifurcation parameter starting at a value of $\Omega = 0.2$. For each increment of forcing frequency 100 forcing periods were simulated to allow for transient behavior before 20 steady state periods of motion were recorded. For each bifurcation diagram Ω was first increased and then decreased through the full frequency range, in order to capture any regions of hysteretic behavior. From these bifurcation diagrams we can define the periodicity of the solutions as the number of impacts which occur per forcing period.

The bifurcation diagrams are shown in Fig. 4 for a forcing frequency range $\Omega = 0.2 - 2.0$, and a forcing amplitude $A_1 = 0.3$. Figure 4 (a) refers to mass 1, and (b) mass 2. In both cases the lower half of the frequency range $\Omega \approx 0.2 - 1.2$ is dominated by low period motions; primarily period 1 and period 2. In the upper half of the frequency range, more complex dynamics are evident, in particular significant regions of chaotic motion exist.

A series of corresponding time series for this system computed at a range of Ω values are shown in Fig. 4, where the trajectory for mass 1 is shown as a red line and for mass 2 as a blue line. The

type of motion seen for each mass and each of the frequency values is summarized in table 2.

Table 2: Vibro-impact motions for 2dof system

Ω	Mass 1	Mass 2
0.2	Period 1	Period 1
0.4	Period 1	Period 2
0.8	Period 1	Period 1
1.0	Period 1	No Impact
1.2	No Impact	No Impact
1.4	Chaotic	Chaotic
1.5	Period 2	Period 2
1.8	Period 1	No Impact

From table 2 we see that only three types of vibro-impact motion are present, period 1, period 2 and chaos. We see also that the two masses can exhibit different vibro-impact motions simultaneously.

In Figs. 5 (a), (b) and (c) both masses have impacts which occur very close together. However across the frequency range considered the occurrence of double impacts, as defined in Sec. 3.4, is actually quite a rare event. In the data computed for Fig. 4 (at an interval between frequency values of 0.0025) only two double impacts occurred, $\Omega = 0.27$ and $\Omega = 0.435$. It is also worth reiterating that even though both impacts occur within a single numerical time step, Δt , we have yet to encounter any which occur at exactly the same time.

4.4.1 Two dimensional parameter space

Because of the relative simplicity of the dynamics in this case, we can consider regions of different vibro-impact solutions in a two dimensional parameter space, (Ω, A_1) ; forcing frequency and forcing amplitude. The resulting parameter space diagram is shown in Fig. 6. Here we see that the regions of different vibro-impact motion remain in a similar order as forcing amplitude A_1 is varied. To the left of the first line starting at $\Omega = 0.4$ is a range of different solutions starting with non-impacting at $A_1 = 0.2$. And ending with a small region of chatter and sticking motions at $A_1 > 0.8$. The chaotic region has periodic windows within it, and for the most part these are period 1, although for some forcing amplitudes small windows of higher periodic motions are

present and in some cases period doubling cascades lead from periodic to chaotic motion.

4.5 Case (b) unequal constraints of different sign

As a counter example to case (a) we briefly examine the case of unequal constraints with differing sign, $s_1 = -0.3$ and $s_2 = 0.1$. In Fig. 7 we show examples of bifurcation diagrams for the two degree of freedom system with unequal constraints of different sign, computed for a forcing amplitude $A_1 = 0.5$. In Fig. 7 (a) the impact velocity, \dot{x}_1 of mass 1 is shown against forcing frequency, Ω , and in (b) the impact velocity, \dot{x}_2 is shown against frequency. We note that because $s_1 < 0$ the impact velocities for mass 1 are all less than zero, and likewise as $s_2 > 0$ the impact velocities for mass 2 are all greater than zero. A region of sticking motions exist at forcing frequencies, $\Omega < 0.5$, which can be seen from the chatter impact velocities successively decreasing toward zero.

In Fig. 8 steady state time series plots are shown for a range of forcing frequency values across the range shown in Fig. 7. The type of motion seen for each mass and each of the frequency values is summarized in table 3.

It is clear from Fig. 7 and table 3 that this case exhibits a wider and more complex range of dynamics than the example case (a) discussed in Sec. 4.4. At low frequency, $\Omega < 0.5$ periodic sticking motions preceded by complete chatter exist. We refer to these as period infinity periodic motions as an infinite number of instantaneous impacts occur in one period [Budd & Dux 1994; Wagg & Bishop 2001]. Then as Ω is increased past the sticking region, chatter becomes incomplete. For the example shown in Fig. 8 (b), the motion could be considered as incomplete chatter or period 4 vibro-impact motion. Then in the region $0.6 < \Omega < 1.6$, periodic motions up to period 5 predominate with very small regions of non-periodic (i.e. chaotic) motion. Finally in the higher frequency range $\Omega > 1.6$ large regions of chaotic motion coexist with a period 1 solution.

Table 3: Vibro-impact motions for 2dof system

Ω	Mass 1	Mass 2
0.3	Period Infinity	Period Infinity
0.5	Chatter/P4	Chatter/P4
0.8	Period 2	Period 2
1.1	Period 2	Period 3
1.4	Period 1	Period 1

1.7	P1/Chaotic	P1/Chaotic
2.0	P1/Chaotic	P1/Chaotic
2.1	Chaotic/P1	Chaotic/P1

4.5.1 Impact mappings for the two degree of freedom example case (b)

We now consider a selection of impact mappings which occur in the two degree of freedom example case (b). The individual impact mappings are shown in Fig. 9 (a)-(d) for a range of forcing frequency values $\Omega = 0.3 - 2.05$. In Fig. 9 (a) we show the individual impact map for mass 2 during a sticking motion which occurs at $\Omega = 0.3$. The decreasing impact velocity of the line of points on the left hand side of the plot correspond to the complete chatter sequence which precedes sticking.

In Figs. 9 (b)-(d) we show three chaotic impact mappings which occur in case (b). The first (b) occurs at a forcing frequency value of $\Omega = 0.715$, and we have plotted the individual mapping for mass 2. This attractor is composed of three distinct sets of points, which as Ω is increased leads to a period 3 motion. The attractors in 9 (c) and (d) both occur for the same forcing frequency value, $\Omega = 2.05$. In 9 (c) we show the individual attractor for mass 1, and in 9 (d) the individual attractor for mass 2. The attractor in 9 (d) is composed in part of linear sets leading to zero velocity impacts, and has strong similarities with the types of attractor encountered in single degree of freedom impact systems [Budd & Dux 1994]. The attractor in 9 (c) in contrast is less dominated by linear sets. It is interesting to note that a global impact map would simply superimpose the attractors shown in 9 (c) and (d) into a single plot.

4.6 Sticking motion

4.6.1 Numerical examples

A numerically computed example of sticking motion is shown in Fig. 10 (a) with stop distance values $s_1 = -0.3$ and $s_2 = 0.1$, forcing amplitude $A_1 = 0.5$, and forcing frequency $\Omega = 0.2$. The figure shows the displacement of both masses for this set of parameter values. The motion is period infinity steady state motion and each mass has a complete chatter sequence and sticking period during one excitation period. In Fig. 10 (b) we show a close up of the sticking region computed for mass 1. The vertical lines represent the change in explicit solution from Eqs. (7) to Eq. (32) and back to Eqs. (7) after sticking has ended. It is clear from this figure that despite having to

switch between different explicit solutions, the x_2 trajectory is smooth and continuous throughout this time.

A second numerical example is shown in Fig. 11. Here we have computed a sticking orbit for a system where both stops are equal $s_1 = s_2 = 0.31$. It can be seen that mass 1 starts a chatter sequence around $t = 806.5$ and becomes stuck at approximately $t = 810$. Just after $t = 810$ and again at $t \approx 813.5$ mass 2 experiences impacts. This illustrates the case discussed in Sec. 3.3, where additional impacts occur during sticking.

4.6.2 Sticking orbits and identifying the region S

From Sec. 2.3 we can use the relationship $F_p = 0$ to define the boundary in phase space where sticking ends. For example if we consider, for the system shown in Fig. 10, the case when $x_2 = s_2$ such that $\dot{x}_2 = 0$, the trajectories during sticking are restricted to the x_1, \dot{x}_1 space which is \hat{G} for this example. Then by setting Eq. (36) to zero we define the relationship for the end of sticking as $\dot{x} = -(k/c)x_1 + (k/c)s_2 = \dot{x} = -10x_1 + 1$, which defines the exit boundary of the sticking region S which is denoted ∂S . For sticking to exist we know that the condition $F_p s_p > 0$ must apply, which in this case is the region on the positive side of the ∂S . Note also that ∂S includes the point $(0.1, 0)$ which corresponds to the (x_2, \dot{x}_2) values during sticking.

In Fig. 12 we show seven different sticking trajectories in the x_1, \dot{x}_1 (\hat{G}) phase space. Each trajectory corresponds to a forcing frequency value in the range $\Omega = 0.1 - 0.36$ after which sticking motion no longer exists for this set of parameter values. Each sticking trajectory finishes at the end of sticking line ∂S . However, the starting points of the trajectories do not seem to correspond to an obvious or well defined set of points in this example. We also see that a set joining these points would not provide a bound to S as some of the sticking orbits exist outside this region. The higher frequency sticking trajectories $\Omega = 0.3 - 0.36$ can be seen to propagate from an initial starting point in the plane towards ∂S with limited curvature. The lower frequency range sticking orbits however, have a more complex structure. This occurs because the lower frequency orbits have a longer time stuck to the constraint, which means that the sticking orbits are longer in duration, and consequently more oscillations in the reduced dynamics arise, as can be seen in the time series plots shown in Fig. 8.

In the work on sliding orbits by Di Bernardo *et al.* [2001], S was defined using Utkin's equivalent control method [Utkin 1992]. However, in this case only a subset of the system states are restricted to S , with the result that we cannot define S simply in terms of the system parameters alone, we

must include some of the system states. Therefore for this type of system we can at best define S as the region where $F_p s_p > 0$ which is bounded on one side by ∂S .

5 Conclusions

In this paper we have considered the dynamics of multi-degree of freedom impact oscillators with multiple constraints using a two degree of freedom example to illustrate the dynamical complexities of these systems. We have considered the mathematical modelling of these multiply constrained systems using a modal formulation, and developed a modal form of the coefficient of restitution rule to model single, multiple and simultaneous impact events. The concept of individual and global impact maps has been introduced in the context of multiply constrained systems. In addition we have considered sticking solutions which occur in these systems. In Sec. 3 we discussed the techniques for computing solutions for multiply constrained impact systems, including sticking, sticking with multiple impacts and simultaneous impacts.

We have then considered the example of a two degree of freedom impacting system with both masses constrained. For this system we have devised explicit solutions for the two possible sticking cases which occur when $A_2 = 0$. Detailed time series and bifurcation diagrams were considered for two cases of the the two degree of freedom example. In the first case the motion limiting constraints were of equal magnitude and the same sign, and in the second case differing magnitude and opposing sign. The equal magnitude constraints case had dynamics dominated in the low frequency range by low periodic motions, with chaotic motion dominating in the higher frequency range. This was shown to persist for a significant range of forcing amplitude values. The unequal constraints case exhibits more complex dynamics with regions of chatter, sticking and higher periodic motion.

Using the results from the sticking motion analysis we have shown examples of periodic sticking motions and observed that the switching between sticking and non-sticking solutions produces smooth trajectories for the non-sticking mass. We have discussed the evolutions of sticking orbits on the hyperplane \hat{G} and noted that only the exit boundary, ∂S can be defined for this example.

References

- Babitsky, V. I. [1998]. *Theory of vibro-impact systems and applications*. Springer-Verlag: Berlin.
- Bishop, S. R., Thompson, M. G. & Foale, S. [1996]. Prediction of period-1 impacts in a driven

- beam. *Proc. Roy. Soc. London A* **452**, 2579–2592.
- Budd, C. J. & Dux, F. [1994]. Chattering and related behaviour in impact oscillators. *Phil. Trans. Roy. Soc. London A* **347**, 365–389.
- Chatterjee, S., Mallik, A. K. & Ghosh, A. [1995]. On impact dampers for non-linear vibrating systems. *J. Sound and Vibration* **187**(3), 403–420.
- Cusumano, J. P. & Bai, B-Y. [1993]. Period-infinity periodic motions, chaos and spatial coherence in a 10 degree of freedom impact oscillator. *Chaos, Solitons and Fractals* **3**, 515–536.
- Di Benardo, M., Johansson, K. H. & Vasca, F. [2001]. Self-oscillations and sliding in relay feedback systems:symmetry and bifurcations. *Int. J. Bifurcation and Chaos* **4**(11), 1121–1140.
- Galvanetto, U. [2001]. Some discontinuous bifurcations in a two block stick-slip system. *J. Sound and Vibration* **248**(4), 653–669.
- Gladwell, G. M. L. [1986]. *Inverse problems in vibration*. Dordrecht: Kluwer.
- Hogan, S. J. & Homer, M. E. [1999]. Graph theory and piecewise smooth dynamical systems of arbitrary dimension. *Chaos, Solitons and Fractals* **10**(11), 1869–1880.
- Luo, G. W. & Xie, J. H. [1998]. Hopf bifurcation of a two-degree-of-freedom vibro-impact system. *J. Sound and Vibration* **213**, 391–408.
- Luo, G. W. & Xie, J. H. [2002]. Hopf bifurcations and chaos of a two-degree-of-freedom vibro-impact system in two strong resonance cases. *Non-linear Mechanics* **37**, 19–34.
- Masri, S. F. [1972]. Theory of the dynamic vibration neutraliser with motion-limiting stops. *Trans. A. Soc. Mech. Eng., J. Applied Mechanics* **39**, 563–568.
- Meirovitch, L. [1967]. *Analytical methods in vibration*. New York: McGraw-Hill.
- Moon, F. C. & Shaw, S. W. [1983]. Chaotic vibrations of a beam with non-linear boundary conditions. *Int. J. Non-Linear Mechanics* **18**(6), 465–477.
- Natsiavas, S. [1993]. Dynamics of multiple-degree-of-freedom oscillators with colliding components. *J. Sound and Vibration* **165**(3), 439–453.
- Neilson, R. D. & Gonsalves, D. H. [1993]. Chaotic motion of a rotor system with a bearing clearance. In *Applications of fractals and chaos*, A. J. Crilly, R. A. Earnshaw, & H. Jones (Eds.), 285–303. Springer-Verlag.

- Nigm, M. M. & Shabana, A. A. [1983]. Effect of an impact damper on a multi-degree of freedom system. *J. Sound and Vibration* **89**(4), 541–557.
- Pun, D., Lua, S. L., Law, S. S. & Cao, D. Q. [1998]. Forced vibration of a multidegree impact oscillator. *J. Sound and Vibration* **213**(3), 447–466.
- Shaw, J. & Shaw, S. W. [1989]. The onset of chaos in a two-degree of freedom impacting system. *J. Applied Mechanics* **56**, 168–174.
- Shaw, S. W. & Holmes, P. J. [1983]. A periodically forced piecewise linear oscillator. *J. Sound and Vibration* **90**(1), 129–155.
- Theodossiades, S. & Natsiavas, S. [2001]. Periodic and chaotic dynamics of motor-driven gear-pair system with backlash. *Chaos, Solitons and Fractals* **12**, 2427–2440.
- Thompson, J. M. T. & Stewart, H. B. [2002]. *Nonlinear dynamics and chaos*. Chichester: John Wiley.
- Toulemonde, C. & Gontier, C [1998]. Sticking motions of impact oscillators. *Eur. J. Mechanics A:Solids* **17**(2), 339–366.
- Utkin, V. I. [1992]. *Sliding modes in control optimization*. Springer-Verlag.
- Wagg, D. J. & Bishop, S. R. [2001]. Chatter, sticking and chaotic impacting motion in a two-degree of freedom impact oscillator. *Int. J. Bifurcation and Chaos* **11**(1), 57–71.
- Wagg, D. J., Karpodinis, G. & Bishop, S. R. [1999]. An experimental study of the impulse response of a vibro-impacting cantilever beam. *J. Sound and Vibration* **228**(2), 243–264.
- Wen, G-L [2001]. Codimension-2 Hopf bifurcation of a two-degree-of-freedom vibro-impact system. *J. Sound and Vibration* **242**(3), 475–485.

Figure Captions

- Figure 1. Schematic representation of an N degree of freedom impact oscillator with multiple motion limiting constraints.
- Figure 2. Schematic representation of an 2 degree of freedom impact oscillators with motion limiting constraints for both masses: (a) Constraints on same side; (b) constraints on opposite sides.
- Figure 3. Flow diagram of numerical computations for two degree of freedom example
- Figure 4. Numerically computed two degree of freedom impact oscillator bifurcation diagrams for case (a) with impact stops $s_1 = s_2 = 0.3$. Parameter values $m_1 = m_2 = k_1 = k_2 = 1$, $c_1 = c_2 = 0.1$, $r = 0.7$, forcing $A_2 = 0.0$, $A_1 = 0.3$. (a) Impact velocity $\dot{x}_1(t_-)$ vs forcing frequency Ω . (b) Impact velocity $\dot{x}_2(t_-)$ vs forcing frequency Ω .
- Figure 5. Numerically computed time series for a two degree of freedom impact oscillator for case (a) with impact stops $s_1 = s_2 = 0.3$. Red line x_1 , blue line x_2 . Parameter values $m_1 = m_2 = k_1 = k_2 = 1$, $c_1 = c_2 = 0.1$, $r = 0.7$, forcing $A_2 = 0.0$, $A_1 = 0.3$. (a) $\Omega = 0.2$ (b) $\Omega = 0.4$; (c) $\Omega = 0.8$; (d) $\Omega = 1.0$ (e) $\Omega = 1.2$; (f) $\Omega = 1.4$; (g) $\Omega = 1.5$; (h) $\Omega = 1.8$.
- Figure 6. Regions of vibro-impact motion for case (a) in a two dimensional parameter space, (Ω, A_1) . Parameter values as for case (a), NI denotes No Impact.
- Figure 7. Numerically computed two degree of freedom impact oscillator bifurcation diagram for case (b) with impact stops $s_1 = -0.3, s_2 = 0.1$. Parameter values $m_1 = m_2 = 1$, $k_1 = k_2 = 1$, $c_1 = c_2 = 0.1$, $r = 0.7$, forcing $A_2 = 0.0$, $A_1 = 0.5$. (a) Impact velocity $\dot{x}_1(t_-)$ vs forcing frequency Ω . (b) Impact velocity $\dot{x}_2(t_-)$ vs forcing frequency Ω .
- Figure 8. Numerically computed time series for a two degree of freedom impact oscillator for case (b) with impact stops $s_1 = -0.3, s_2 = 0.1$. Red line x_1 , blue line x_2 . Parameter values $m_1 = m_2 = k_1 = k_2 = 1$, $c_1 = c_2 = 0.1$, $r = 0.7$, forcing $A_2 = 0.0$, $A_1 = 0.5$. (a) $\Omega = 0.3$ (b) $\Omega = 0.5$; (c) $\Omega = 0.8$; (d) $\Omega = 1.1$ (e) $\Omega = 1.4$; (f) $\Omega = 1.7$; (g) $\Omega = 2.0$; (h) $\Omega = 2.1$.
- Figure 9. Two degree of freedom impact oscillator impact maps for case (b). Parameter values $m_1 = m_2 = 1$, $k_1 = k_2 = 1$, $c_1 = c_2 = 0.1$, $r = 0.7$, $A_2 = 0.0$, $A_1 = 0.5$. (a) $\omega = 0.3$ velocity= \dot{x}_2 , (b) $\omega = 0.715$ velocity= \dot{x}_2 (c) $\omega = 2.05$ velocity= \dot{x}_1 , (d) $\omega = 2.05$ velocity= \dot{x}_2 .

- Figure 10. Numerically computed displacement-time series of a two degree of freedom impact oscillator with constraints $s_1 = -0.3$ and $s_2 = 0.1$; Red line mass 1; blue line mass 2. (a) showing chatter and sticking motion. (b) close up of the sticking and chatter region for mass 1. The vertical dashed lines indicate the region of explicit sticking solution.
- Figure 11. Numerically computed displacement-time series of a two degree of freedom impact oscillator showing additional impacts during sticking with constraints $s_1 = s_2 = 0.31$; Red line mass 1; blue line mass 2.
- Figure 12. Sticking trajectories in the range $\Omega = 0.1 - 0.36$ showing the end of sticking boundary represented in this example as the line $\dot{x}_1 = -10x_1 + 1$.

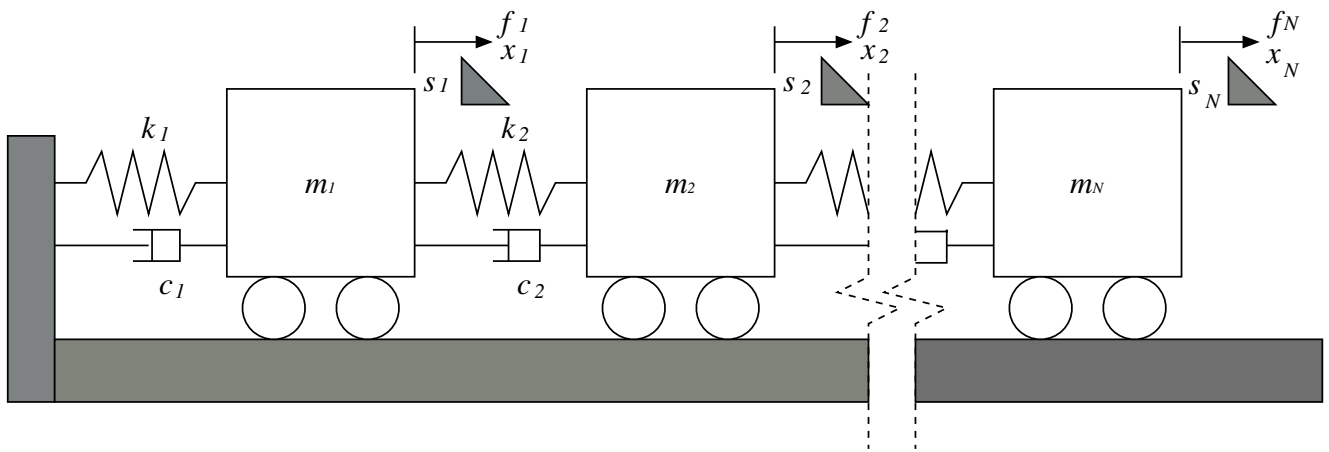
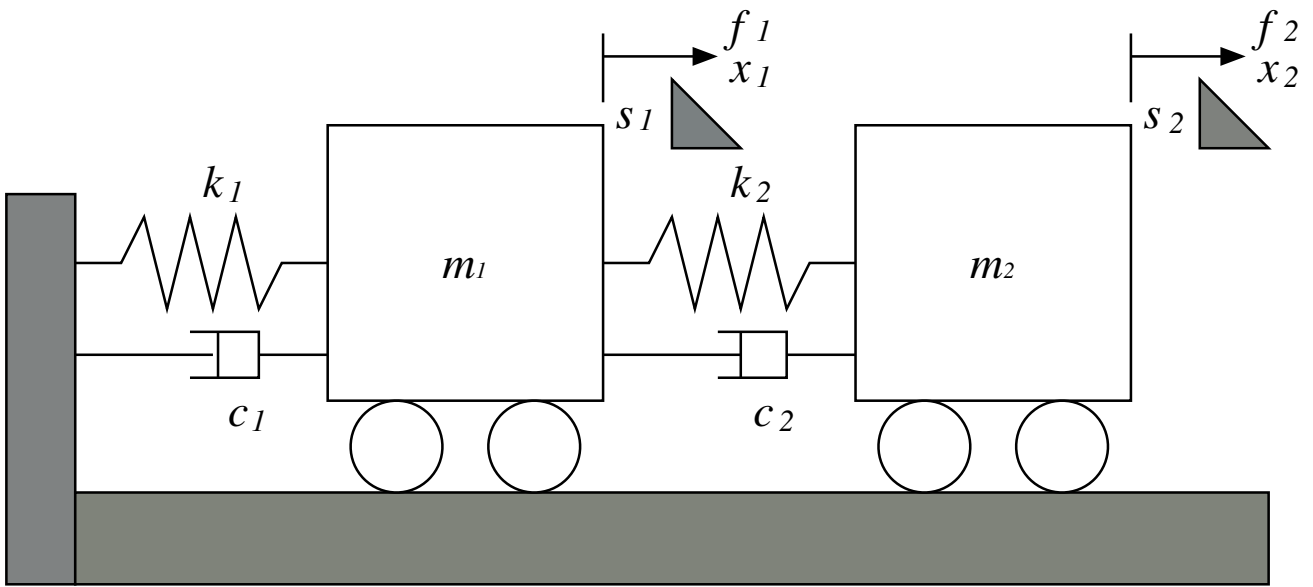
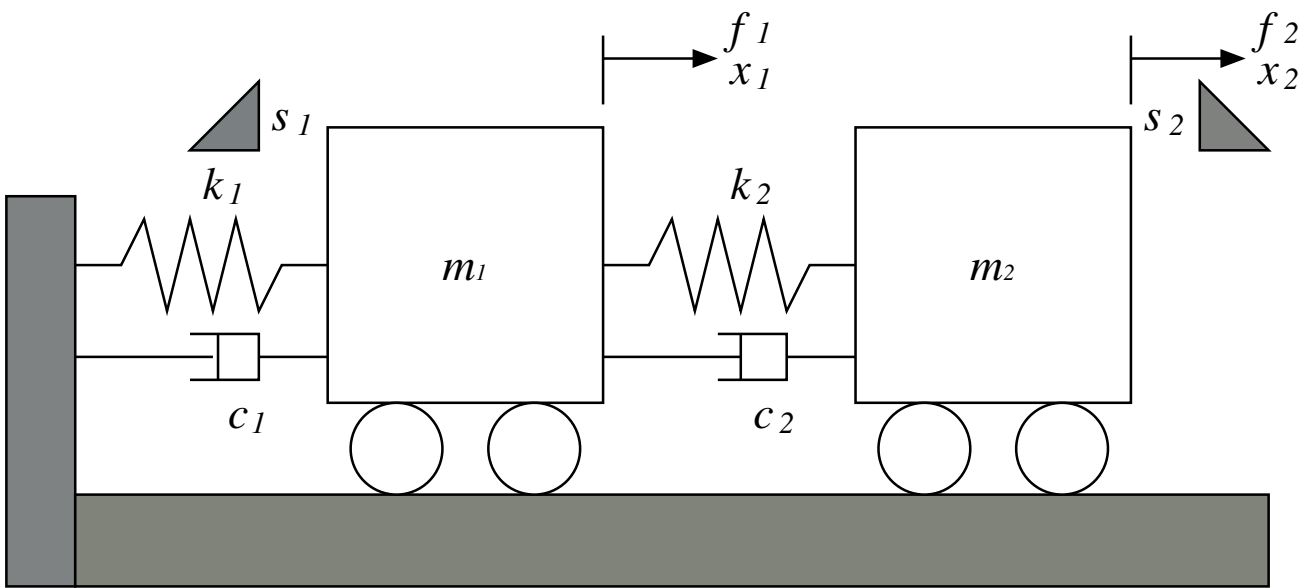


Figure 1:

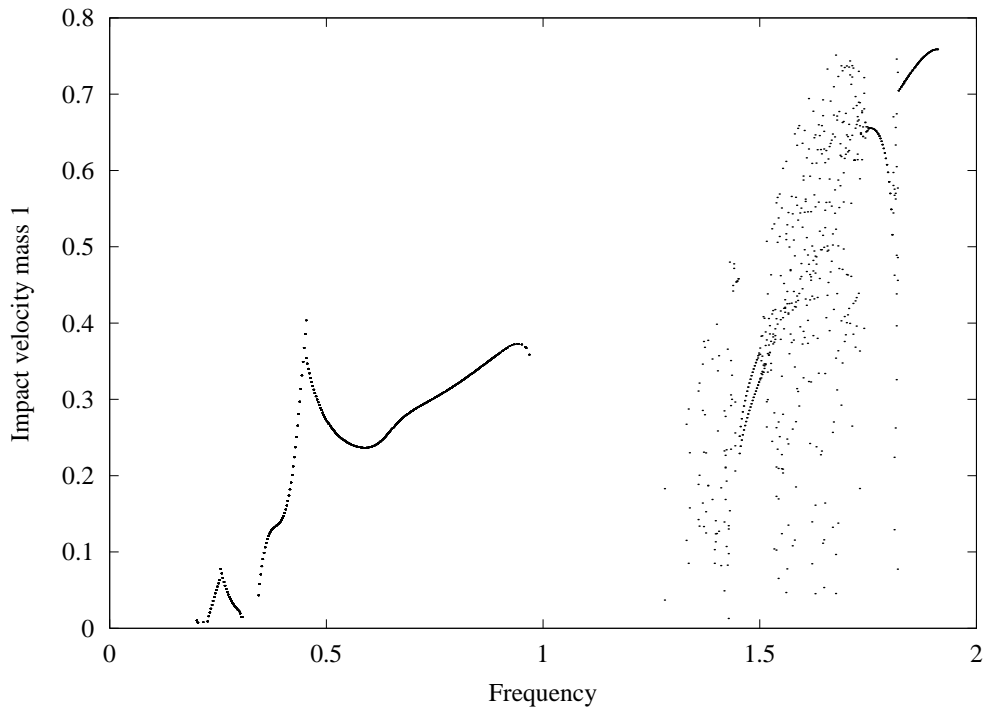


(a)

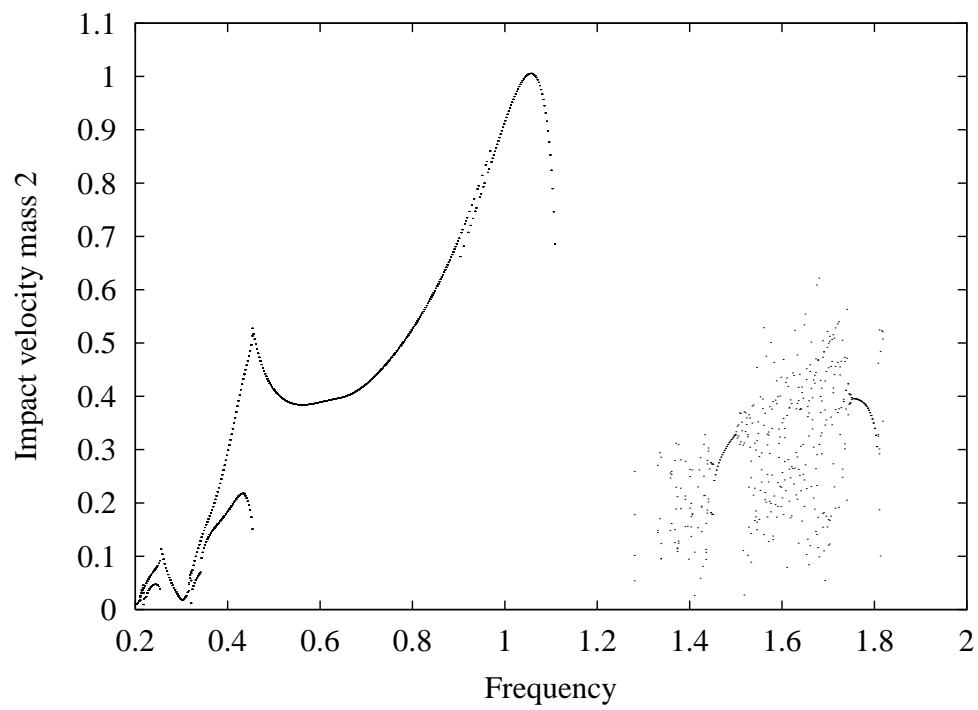


(b)

Figure 2:



(a)



(b)

Figure 4:

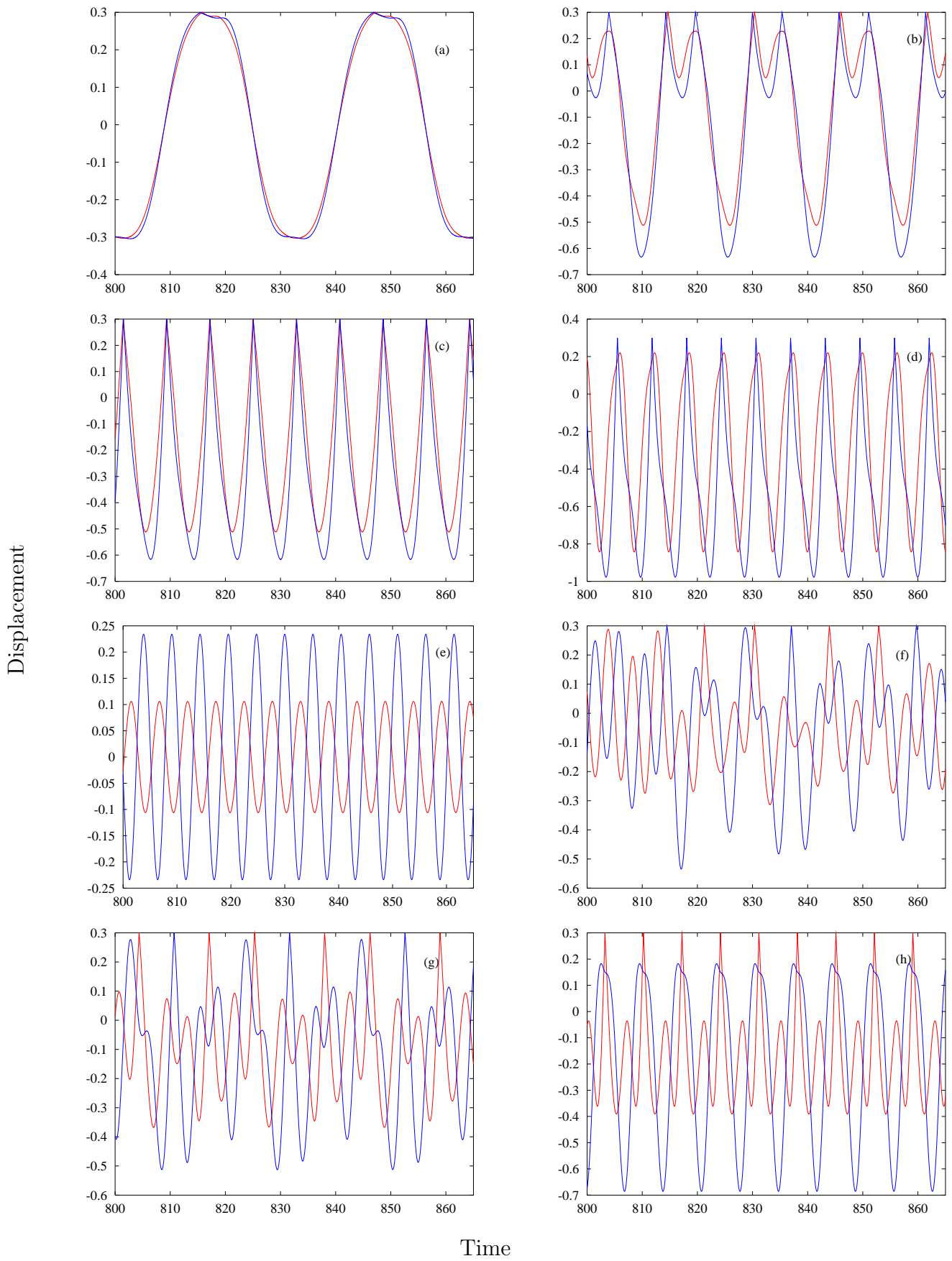


Figure 5:

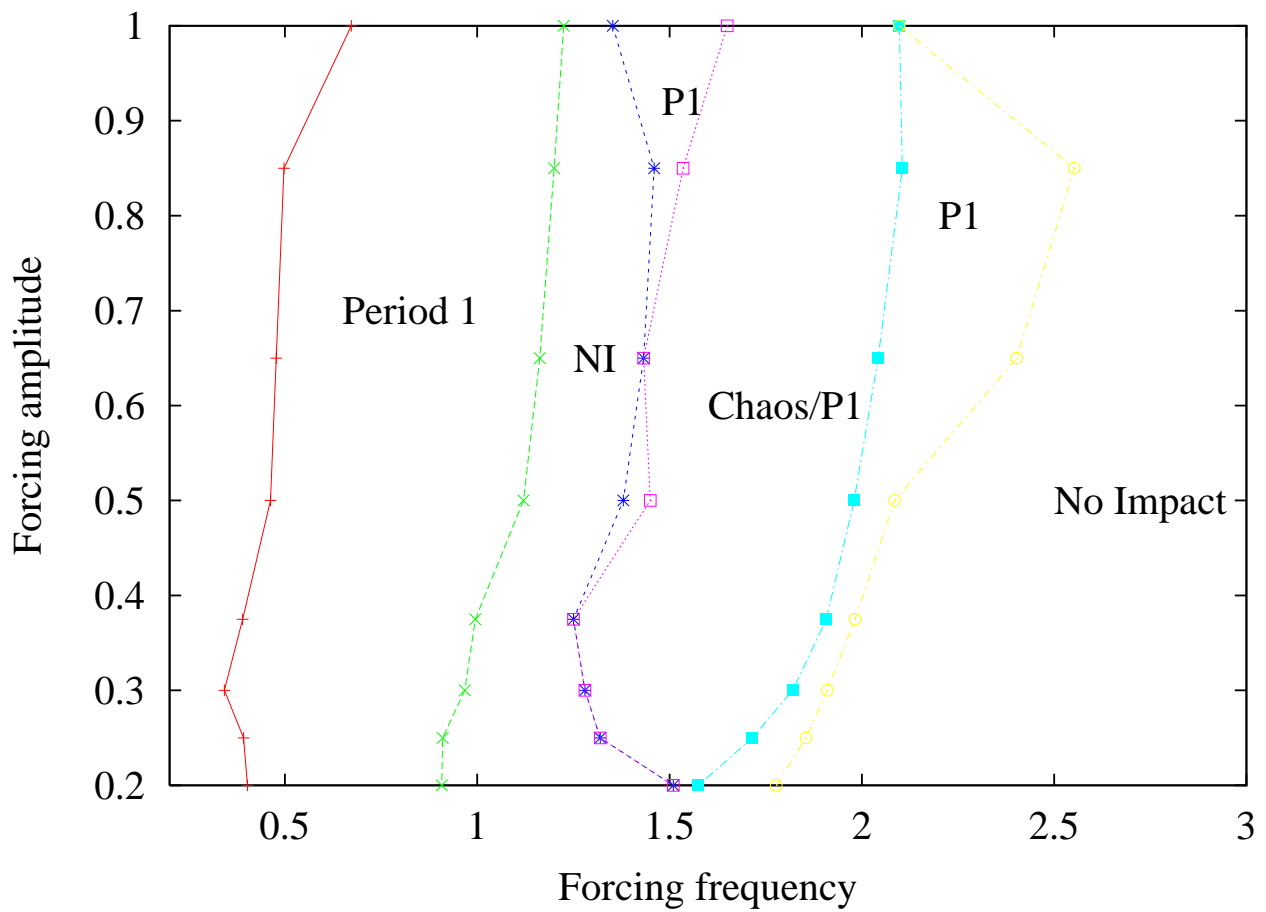
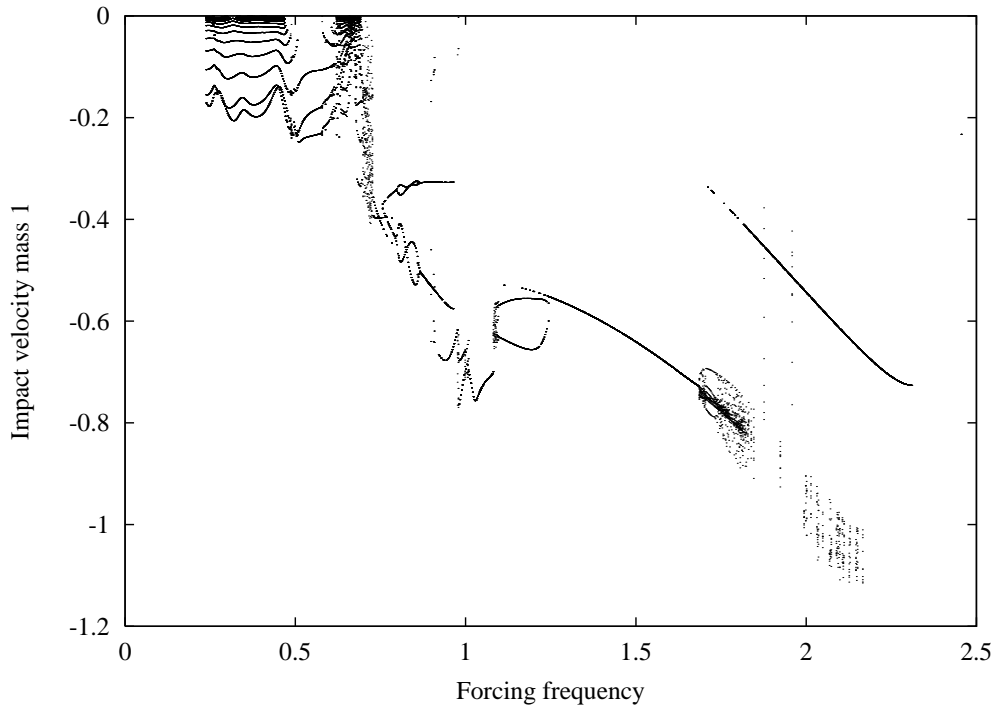
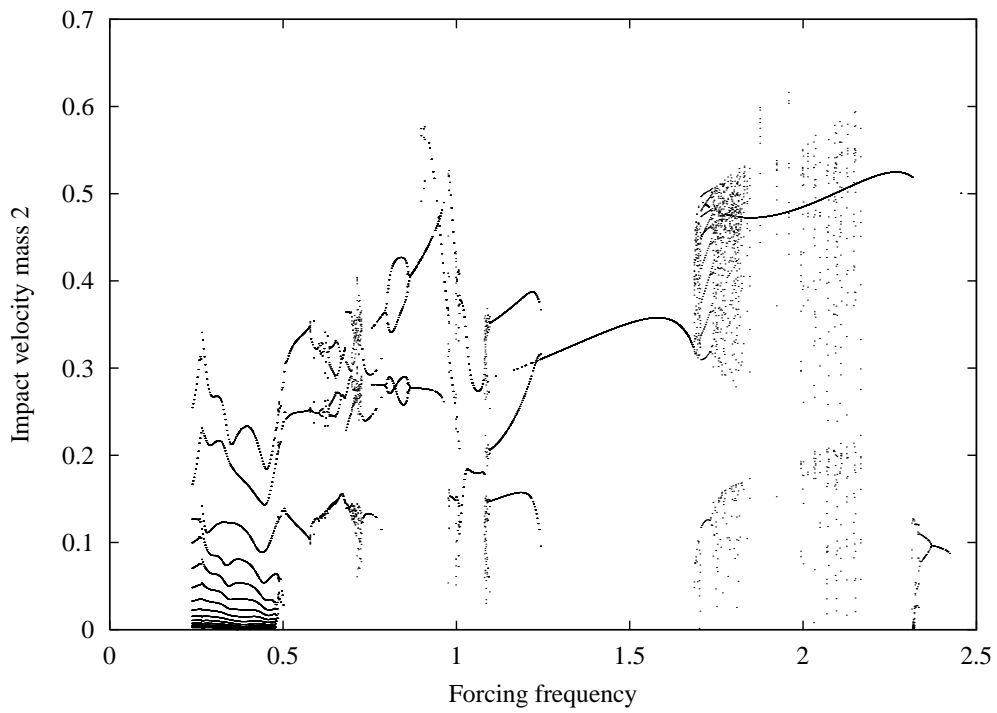


Figure 6:



(a)



(b)

Figure 7:

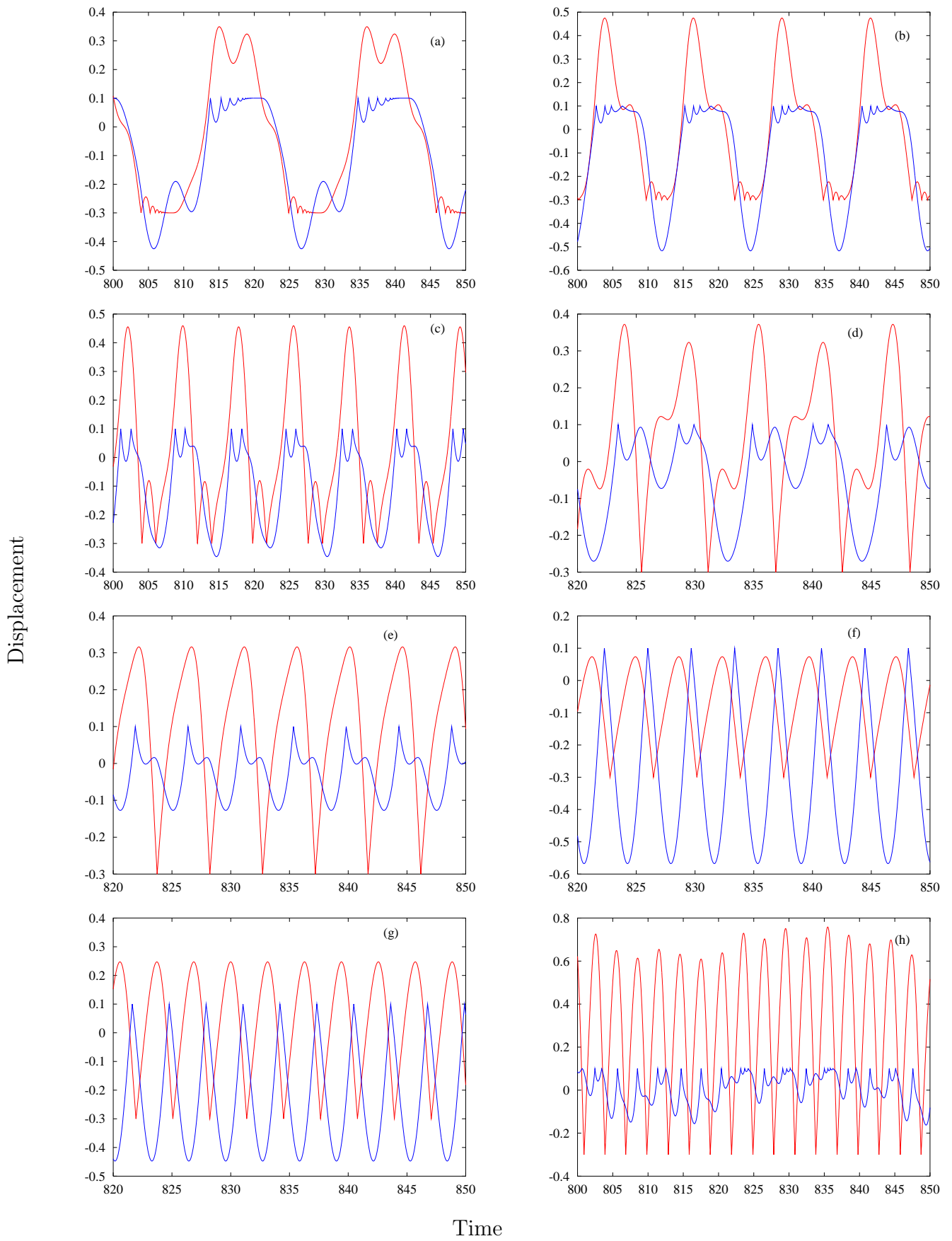


Figure 8:

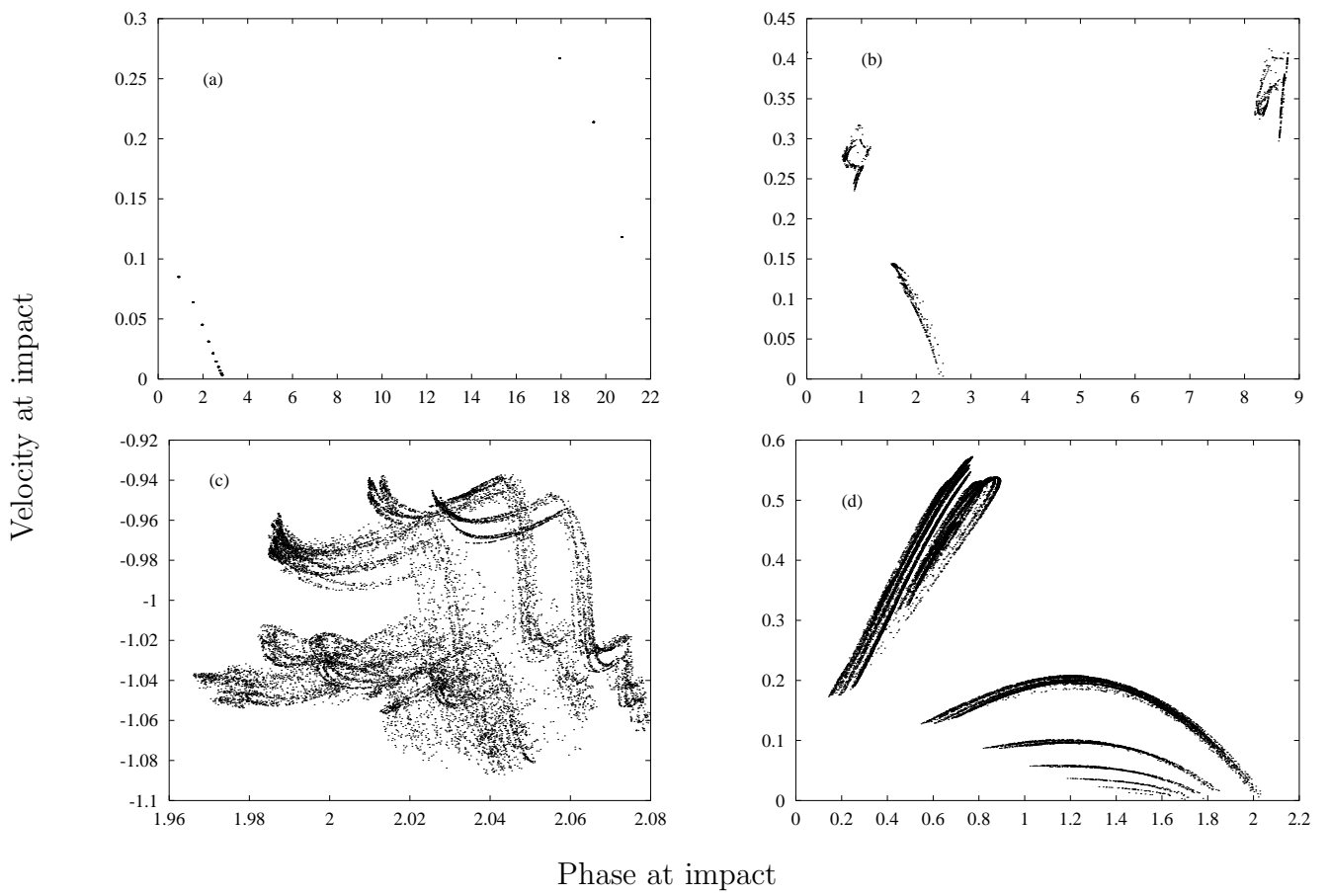
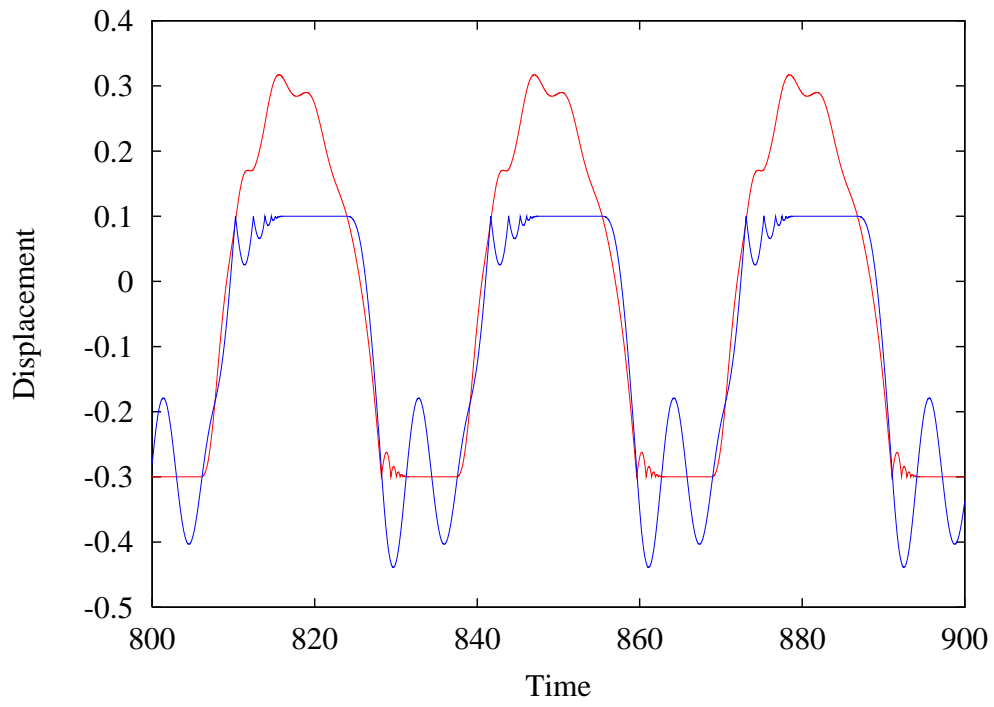
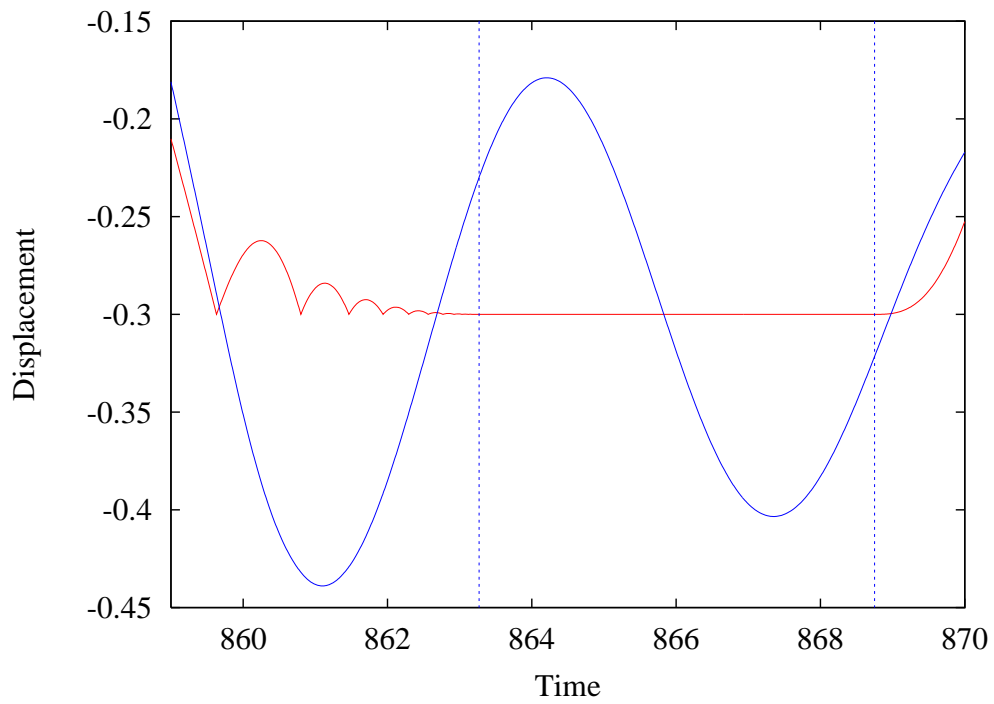


Figure 9:



(a)



(b)

Figure 10:

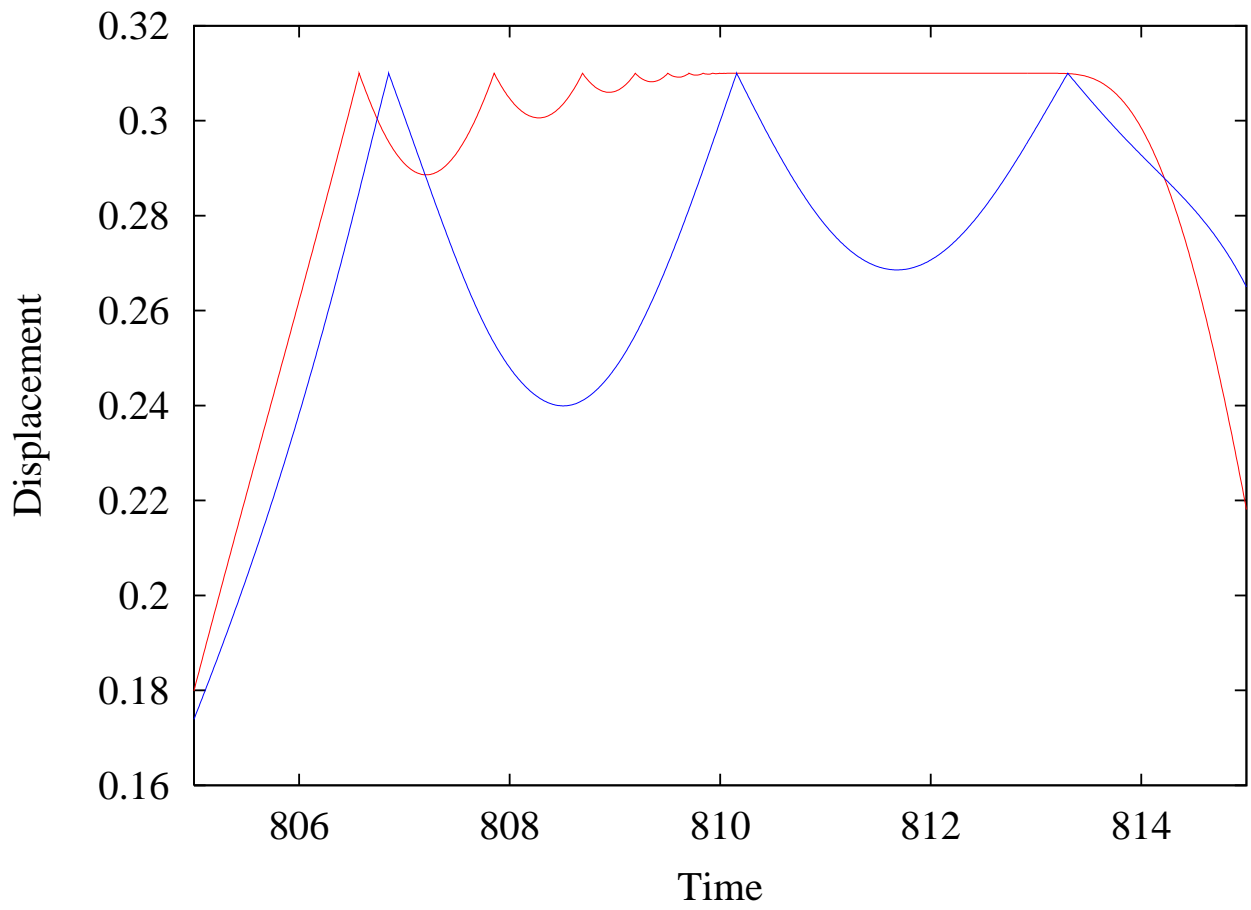


Figure 11:

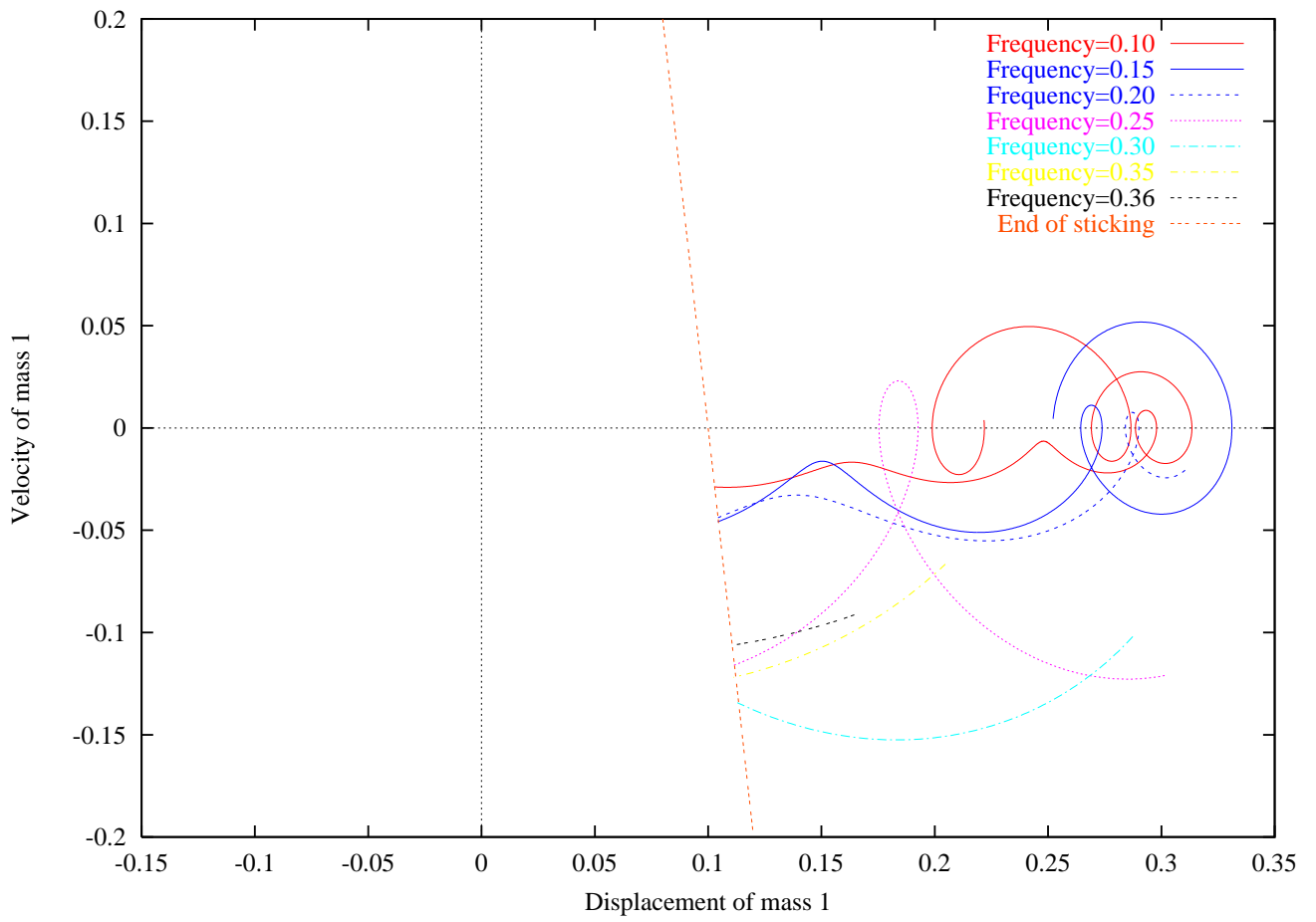


Figure 12: